IN-39

97840

P.18

NASA
Technical
Paper
3248

June 1992

Effect of Type of Load on Stress Analysis of Thin-Walled Ducts

J. B. Min
and P. K. Aggarwal

NASA

NASA
Technical
Paper
3248

1992

Effect of Type of Load on Stress Analysis of Thin-Walled Ducts

J. B. Min
and P. K. Aggarwal
George C. Marshall Space Flight Center
Marshall Space Flight Center, Alabama

National Aeronautics and
Space Administration
Office of Management
Scientific and Technical
Information Program

TABLE OF CONTENTS

LIST OF ILLUSTRATIONS

TECHNICAL PAPER

EFFECT OF TYPE OF LOAD ON STRESS ANALYSIS OF THIN-WALLED DUCTS

I. INTRODUCTION

The standard procedure for qualifying the design of duct (pipe) systems in the space shuttle main engine (SSME) has been fairly well defined. However, since pipe elbows are quite common and important in the SSME duct systems, a clear understanding of the detailed stress profile of these components is necessary for accurate structural and life assessments. The analytical work on the analysis of pipe bends was originated by Von Karman[1] and continued by several researchers[2 3] for decades. In recent years, notable contributions on this topic have been made by Spence and Thompson,[4] Thomson and Spence,[5] Whatham and Thompson,[6] Whatham,[7] Karbin, Rodabaugh, and Whatham,[8] and Natarajan,[9] using the shell theory and finite element method (FEM). However, all these analyses provide limited information about the stress distributions at the interface of the elbow with the straight pipes (tangent point). In general, the weld location at the tangent point is the most critical location governing the design of duct systems. This is especially true in the design of SSME duct systems because of the harsh environment (high pressure/temperature), large dynamic loads, and weld discontinuity (mismatch/weld bead). A space vehicle design also requires optimization of weight for maximum lift-off capability, thus resulting in thin-walled duct systems. Additionally, hot fire data from the strain gauges mounted in the vicinity of these welds are used to anchor these data to the dynamic models for predicting the loads at other locations. Based on the previous studies mentioned above, it is well known that the circumferential and longitudinal stresses at the cross section of the elbow midsection do not peak at the same location. Furthermore, the location (position angles of cross section, fig. 1) of peak stress of these stresses is not at the expected position angle. Therefore, this study was initiated to predict the stress profile at/near the tangent point along the cross section of the duct under various types of loads. Also, similar to the studies done in references 11 and 13 for the midsection of elbow, this study was further extended to understand the stiffening effect on stresses due to pressure at the tangent point. The main objective of this study was to identify the importance of selecting proper locations for mounting strain gauges and utilizing the obtained results to anchor dynamic models for accurate structural and life assessments of the SSME ducts under dynamic environment. The finite element method was utilized in this study as used in references 9, 11, and 12.

II. FINITE ELEMENT MODEL

The finite element models of a 90° elbow with ends terminated by tangent pipes were constructed using the ANSYS isoparametric quadrilateral shell elements.[10] The geometric dimensions, boundary conditions, and loadings were taken from a model analyzed in the literature[11–13] to assure the validity of a finite element model used in this study. The basic assumptions of homogeneous, isotropic thin shells within the range of linear elastic behavior were also used in this study. The models have a ratio of R/r, r/t, and pipe factor (Rt/r^2) of 3.0, 29.13, and 0.103, respectively, where R, r, and t represent the bend radius of curved pipe, mean cross-section radius of curved pipe, and pipe-wall thickness, respectively. In the model, an element aspect ratio was approximately 2:1 for tangent pipes and 1:1 for elbow. Figure 1 illustrates the geometry, loading axes, and sign conventions for the analysis models. A three-dimensional finite element model contains 1,408 shell elements and 4,208 nodes with six degrees of freedom at each node shown in figures 2 and 3. One end of the tangent was fixed, and nodal forces for each loading case were applied at the other end. The moment (1.737×10^6 in-lb) used in references 11 to 13 was taken. In addition, internal hoop stress pressure (p = 26.66 lb/in^2)[11] equivalent to the net pressure (800 lb/in^2)[13] obtained from the relationship $15.0\times p/0.5$ = 800 lb/in^2) was also applied to all elements to simulate the pressure stiffening effect. For simplicity, nominal bending moments were applied by means of a statically equivalent, linearly varying, axial nodal loading pattern as used in references 14 and 15. Similarly, torsional moment was applied by means of a statically equivalent tangential nodal loading pattern.[14 15] In the area of the tangent pipe, away from the applied loads, nominal bending and torsional stresses calculated by the fundamental formula, Mr/I for bending and Mr/J for torsion, were observed, where I and J are a second moment of inertia and a polar moment of inertia, of pipe cross section, respectively. Also, it was observed that the stress profiles due to in-plane bending moment (figs. 4 and 5) at elbow midsection were similar to those given in references 11 and 13. These observations verified the validity of the finite element model and loading application technique used in this study.

III. EFFECT OF TYPES OF LOADS

The nodal stresses in the longitudinal and circumferential directions on the outside and inside shell surfaces were computed for each loading condition. From these computed stresses, the non-dimensional stress intensification factors along the cross sections of the duct were calculated. A stress intensification factor is defined as the ratio of calculated stress intensity at a point to the nominal stress in a piping component. Nominal stress is defined as Mr/I and Mr/J for bending and torsion, respectively. From the analyses, the computed circumferential (hoop) and longitudinal (axial) stresses, in terms of the stress intensification factors, at section BB (fig. 1) are presented in figures 4 through 10. The results/observations for each loading condition are discussed in the following subsections.

3.1 In-Plane Bending Moment (M_z)

The longitudinal and circumferential nodal stresses on the inside and outside surfaces at sections AA and BB were computed. As shown in figures 4 and 5 for section AA, the maximum circumferential and longitudinal stresses occurred on the inside surface at 0° and outside surface at 11.25°, respectively. The circumferential stress factor was larger than the longitudinal stress factor. Also, in this case the finite element analysis results were compared with those derived in references 11, 13, and 16, and good agreements were obtained. Whereas, at section BB shown in figures 6 and 7, the maximum circumferential and longitudinal stresses occurred on the inside surfaces at 0° and 22.5°, respectively. It was also observed that at this section the maximum longitudinal stress was larger than the maximum circumferential stress.[3] As shown in table 1, the position angles of maximum circumferential stresses were the same between sections AA and BB. However, the position angles of the maximum longitudinal stresses were different between sections AA and BB. These observations highlight the importance of selecting the proper locations for the mounting of the strain gauges at the tangent point.

3.2 Out-of-Plane Bending Moment (M_y)

At section BB, as shown in figures 8 and 9, it was found that the maximum circumferential and longitudinal stresses occurred on the outside surface at –45° and on the inside surface at –11.25°, respectively. Similarly to in-plane bending moment, the maximum longitudinal stress factor was larger than the maximum circumferential stress factor. However, comparison of figures 6 and 7 with figures 8 and 9 identified that the maximum circumferential stress factor for out-of-plane bending moment was larger than that of in-plane bending moment. However, the maximum longitudinal stress factor of out-of-plane bending moment was smaller than that of in-plane bending moment. This comparison shows that the results obtained at section BB are contrary to those obtained in section AA as given in reference 16.

3.3 Torque (M_x)

Similarly to the out-of-plane bending moment, since a pure torsional moment exits only on one tangent pipe at the end of the elbow, any additional steps are not needed to calculate the stress factors at section BB. In this load case, the maximum shear stress intensification factor was observed on the outside surface at 0° as shown in figure 10. In general, the stress factor obtained from a finite element model agreed well with the currently used value given in the ASME section III code.[17]

3.4 Effect of Internal Pressure (M_z+p)

The stiffening effect of internal pressure on the flexibility and stress factors of elbow mid-section has been studied and reported in references 4, 6, 11, 12, and 13. However, as mentioned earlier, these studies did not address the effect of bend stiffening at the tangent point. In this study, the resulting stresses were compared to those of cases subjected to moment loads alone to see the effect of internal pressure. However, only the in-plane bending moment case is described since the conclusive results were not observed from the out-of-plane bending and torsional moment cases. At section AA, the finite element analysis results showed an extremely good agreement with the test results given in references 11 and 13. Although this combined load produced lower stress factors compared to those of in-plane bending moment alone, the basic stress profiles were similar at sections AA and BB for both the cases as shown in figures 4 through 7. From this observation, it was concluded that internal pressure stiffening effect at section BB also results in reduced bending stress at section AA.[13] The position angle of maximum stress components is also shown in table 1. As shown in this table, contrary to section AA, the maximum longitudinal stress at section BB occurred on the outside surface.

IV. CONCLUSIONS

In general, a design of duct systems does not require a detailed knowledge of stress profile along the cross section at the tangent point. However, for the duct system in space vehicles a clear understanding of stress profiles at the weld location (tangent point) is required since it operates under the harsh environment and large dynamic loads. Additionally, it does not have the liberty to be over-designed because of the weight penalty. Therefore, this study was conducted using the finite element models and, consequently, the detailed stress profiles along the cross section at the tangent point of a 90° elbow subjected to various types of loads were obtained.

The results show that a lack of the knowledge of detailed stress profile and peak stress location (position angle) for the different types of loads might result in erroneous structural and life predictions. In general, since the dynamic models used to predict the loads are anchored with the strain gauges data obtained from the "hot-fired" systems, the observations of the position angles of maximum stress components are believed to be the most useful finding from this study. In other words, it means that the strain gauges mounted, in general, at 0, 90, 180, and 270° locations will underpredict the strains which may overpredict the fatigue life. Also, it is worth mentioning here that although the 30-in diameter duct was modeled in this study, the results obtained here are basically applicable for other 90° elbows terminated by tangent pipes with similar ratio(s) of R/r, r/t, and Rt/r^2.

REFERENCES

1. Von Karman, T.: "Uer die Formanderung dunnwandiger Rohre insbeson ders federnder Ansgleichrohe," vol. 55, Zeitschrift VDI, 1911.

2. Dodge, W.G., and Moore, S.E.: "Stress Indices and Flexibility Factors for Moment Loadings on Elbows and Curved Pipe." Welding Research Council Bulletin, 179, December 1972.

3. Imamasa, J., and Uragami, K.: "Experimental Study of Flexibility Factors and Stresses of Welding Elbows With End Effects." Second International Conference on Pressure Vessel Technology, San Antonio, Texas, October 1973.

4. Spence, J., and Thomson, G.: "Flanged Pipe Bends Under Combined Pressure and In-Plane Bending." Intr. Conf. on Pressure Vessel Technology, vol. 1, San Francisco, September 9–14, 1984.

5. Thomson, G., and Spence, J.: "Maximum Stress and Flexibility Factors of Smooth Pipe Bends With Tangent Pipe Terminations Under In-Plane Bending." J. of Pressure Vessel Technology, vol. 105, November 1983, pp. 329–336.

6. Whatham, J.F., and Thompson, J.J.: "The Bending and Pressurizing of Pipe Bends With Flanged Tangents." Nuclear Engineering and Design 54, 1979, pp. 17–28.

7. Whatham, J.F.: "Pipe Bend Analysis by Thin Shell Theory." J. of Applied Mechanics of Trans. of the ASME, vol. 53, March 1986, pp. 173–180.

8. Karabin, M.E., Rodabaugh, E.C., and Whatham, J.F.: "Stress Component Indices for Elbow-Straight Pipe Junctions Subjected to In-Plane Bending." J. of Pressure Vessel Technology, vol. 108, February 1986, pp. 86–91.

9. Natarajan, R.: Letter to the Editor, J. Pressure Vessel Technology, vol. 107, February 1985, pp. 5–6.

10. ANSYS Rev. 4.4, User's Manuals, vol. I and II, 1989.

11. Natarajan, R., and Mirza, S.: "Effect of Internal Pressure on Flexibility Factors in Pipe Elbows With End Constraints." J. of Pressure Vessel Technology, vol. 107, February 1985, pp. 60–63.

12. Natarajan, R., and Mirza, S.: "Effect of Thickness Variation on Stress Analysis of Piping Elbows Under Internal Pressure." Computers & Structures, vol. 18, No. 5, 1984, pp. 767–778.

13. Rodabaugh, E.C., and George, H.H.: "Effect of Internal Pressure on Flexibility and Stress-Intensification Factors of Curved Pipe or Welding Elbows." Trans. of the ASME, May 1957, pp. 939–948.

14. Tso, F.K.W., and Weed, R.A.: "Stress Analysis of Cylindrical Pressure Vessels With Closely Spaced Nozzles by the Finite Element Method." NUREG/CR-0507, May 1979.

15. Lewis, G.D., and Chao, Y.J.: "Flexibility of Trunnion Piping Elbows." J. of Pressure Vessel Technology, vol. 112, May 1990, pp. 184–187.

16. Pardue, T.E., and Vigness, I.: "Properties of Thin-Walled Curved Tubes of Short-Bend Radius." Trans. of the ASME, January 1951, pp. 77–87.

17. ASME Boiler and Pressure Vessel Code, Section III, "Nuclear Power Plant Components," ASME, New York, 1989 Edition.

Table 1. Position angles of maximum stress components at sections AA and BB.

Sections / Loads	Position Angles of Max. Stress Section AA			Position Angles of Max. Stress Section BB		
	Hoop	Axial	Fig. No.	Hoop	Axial	Fig. No.
+Mz	0.00 (inside surface)	11.25 (outside surface)	4, 5	0.00 (inside surface)	22.50 (inside surface)	6, 7
+Mz + p	0.00 (inside surface)	11.25 (outside surface)	4, 5	0.00 (inside surface)	22.50 (outside surface)	6, 7
- My	-	-	-	-45.00 (outside surface)	-11.25 (inside surface)	8, 9
Position Angles of Max. Shear Stress at Section BB						
-Mx	0.00 (outside surface)					10

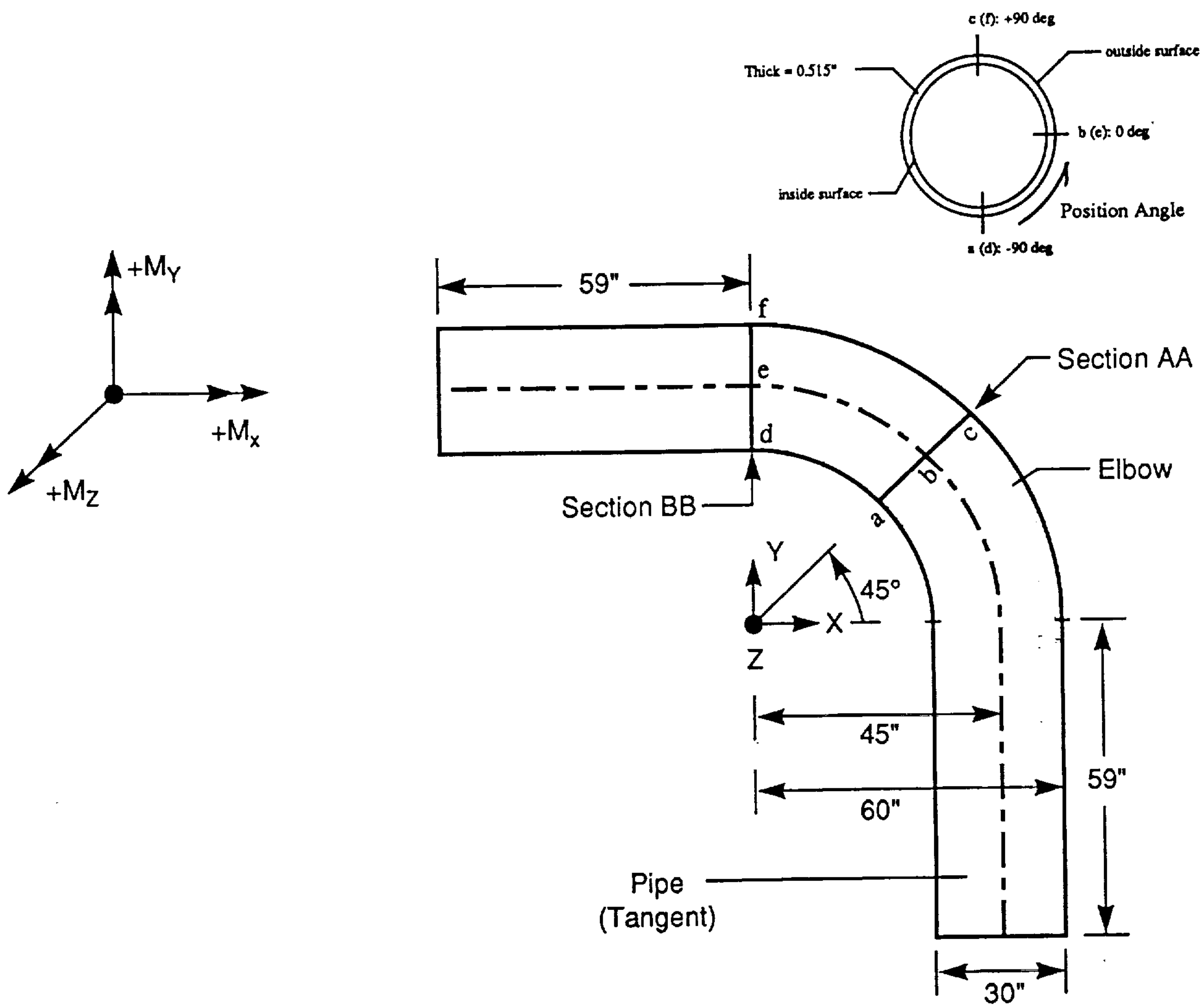

Figure 1. Geometric dimensions of pipe elbow and loading axes (a, b, c, d, e, and f indicate the positions for cross section).

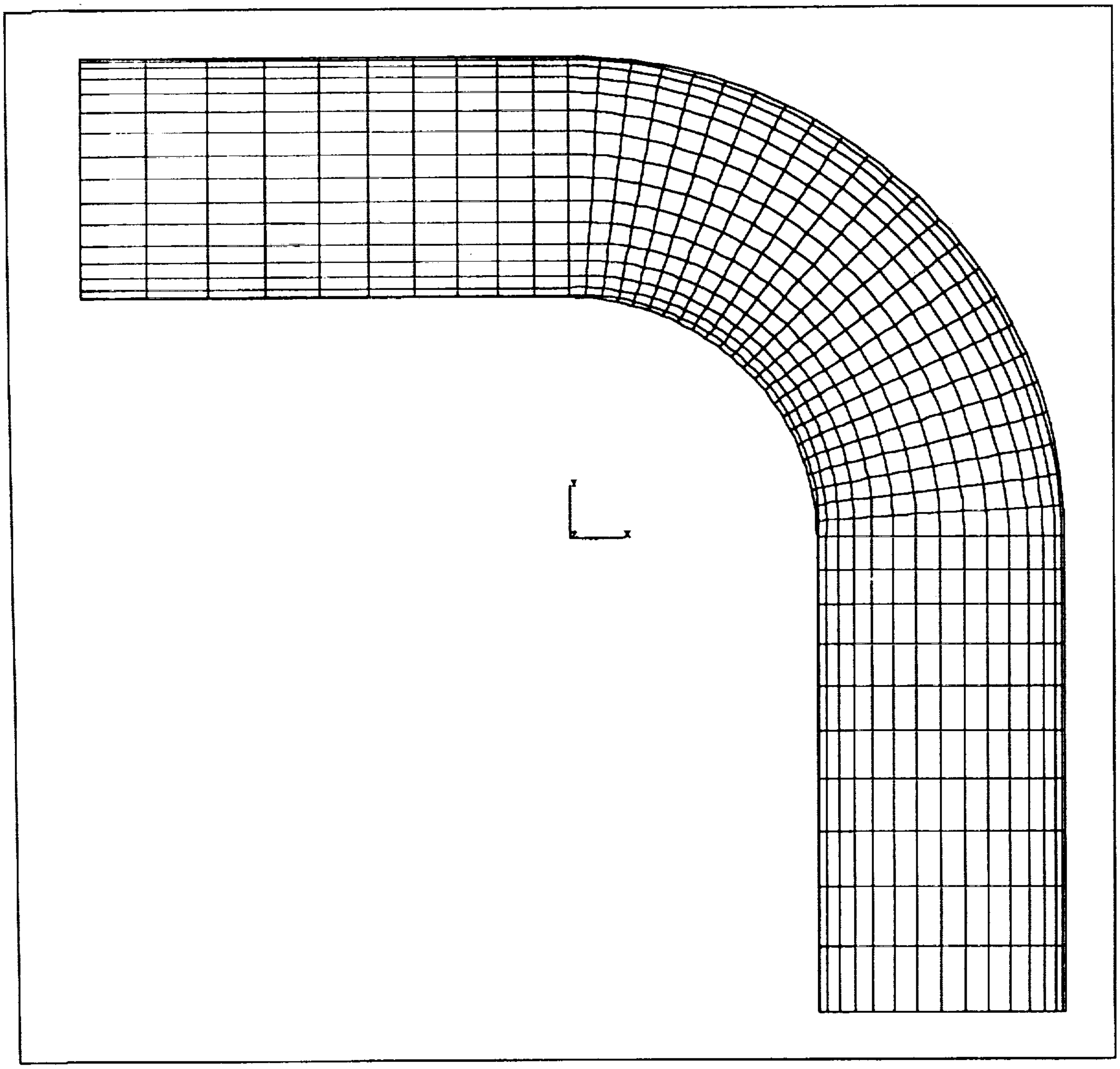

Figure 2. Front view of finite element model.

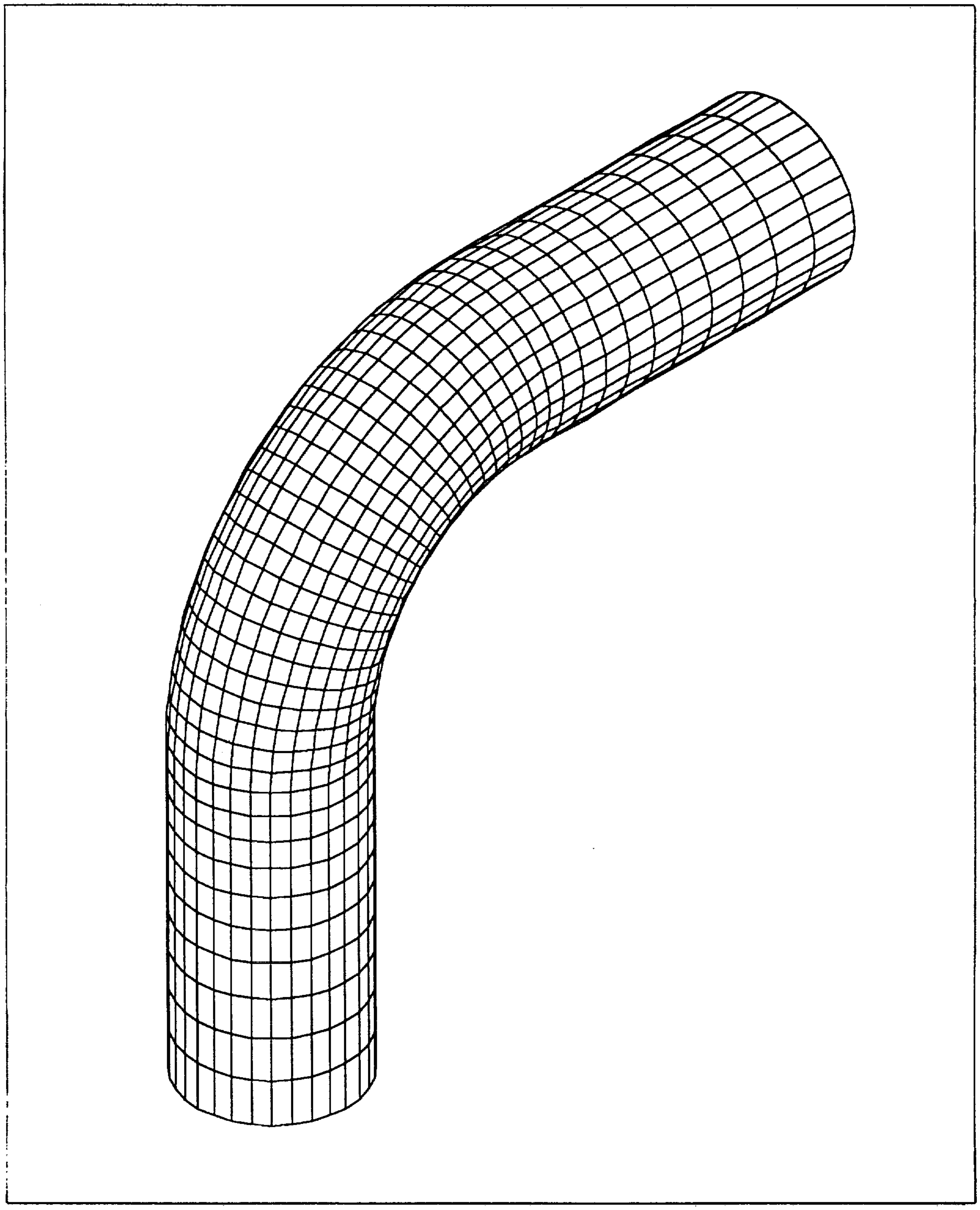

Figure 3. Isometric view of finite element model.

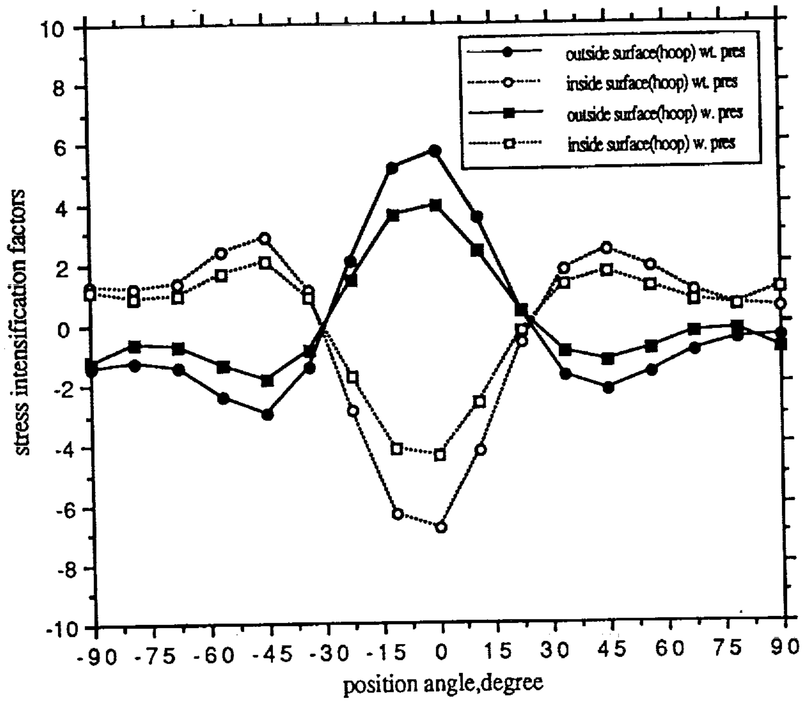

Figure 4. Circumferential stress factors of in-plane bending moment with (w)/without (wt) internal pressure at section AA.

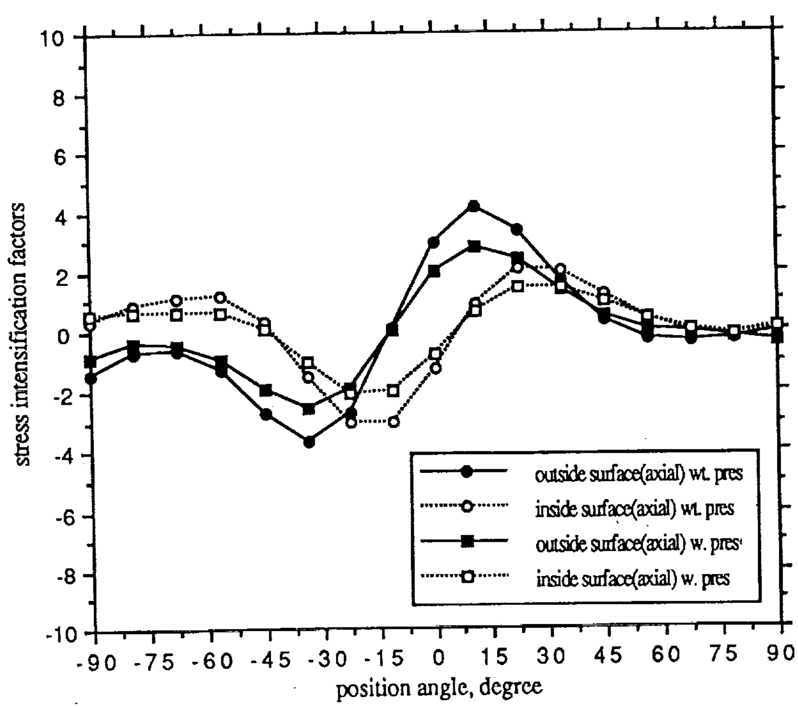

Figure 5. Longitudinal stress factors of in-plane bending moment with (w)/without (wt) internal pressure at section AA.

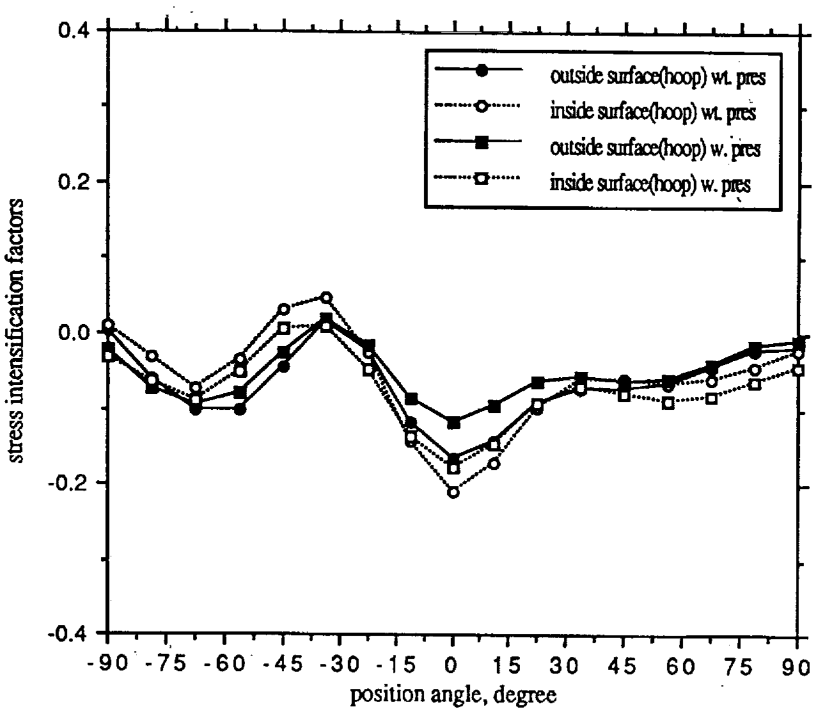

Figure 6. Circumferential stress factors of in-plane bending moment with (w)/with (wt) internal pressure at section BB.

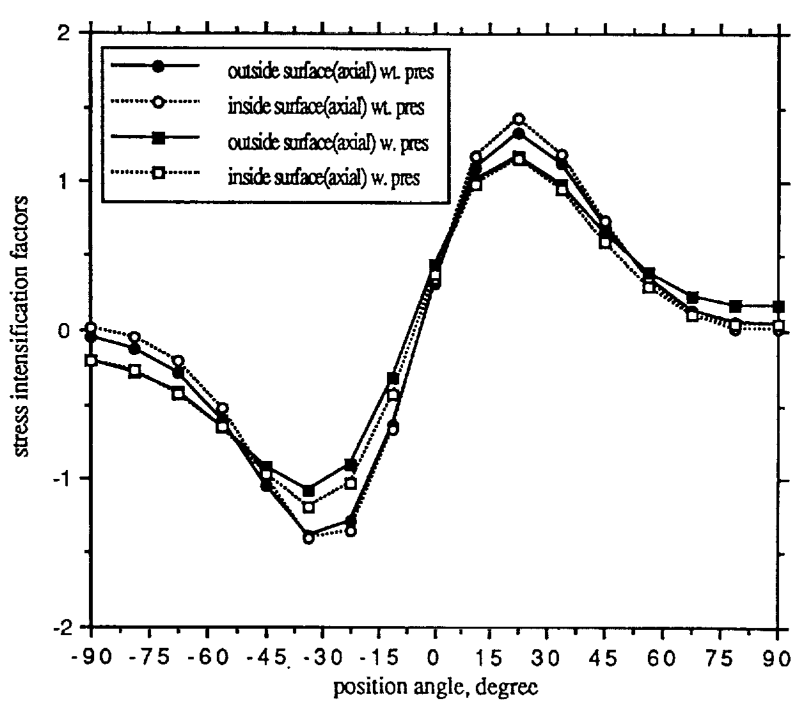

Figure 7. Longitudinal stress factors of in-plane bending moment with (w)/without (wt) internal pressure at section BB.

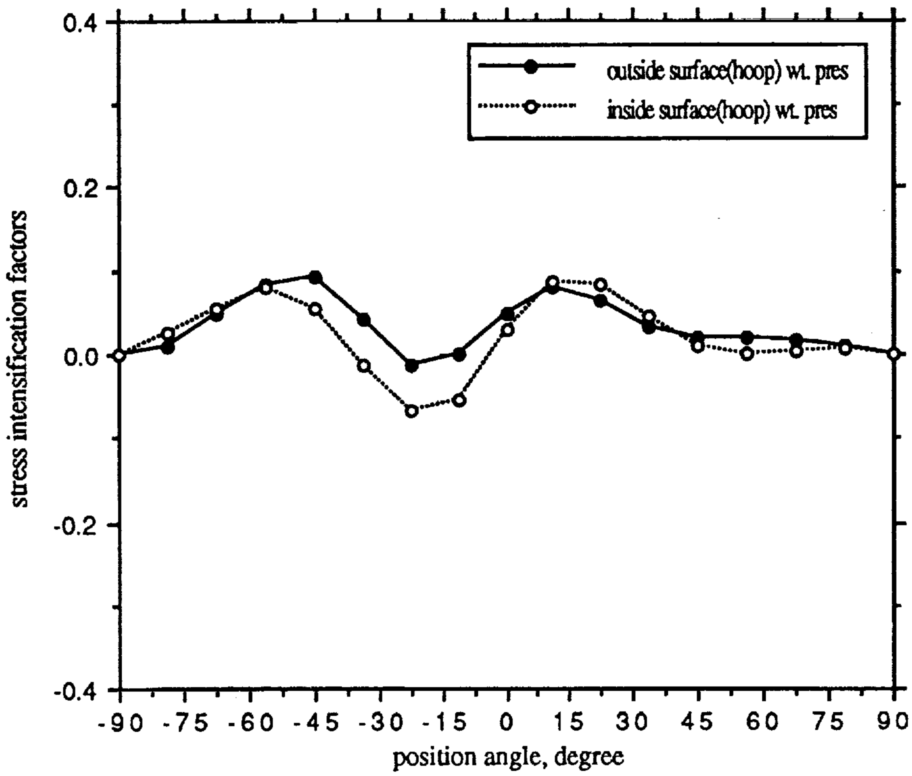

Figure 8. Circumferential stress factors of out-of-plane bending moment without (wt) internal pressure at section BB.

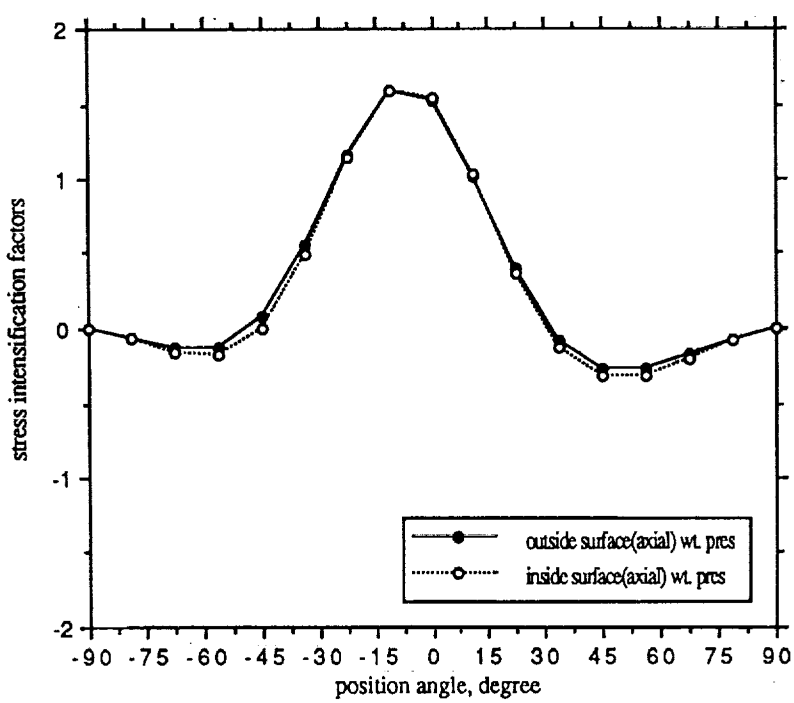

Figure 9. Longitudinal stress factors of out-of-plane bending moment without (wt) internal pressure at section BB.

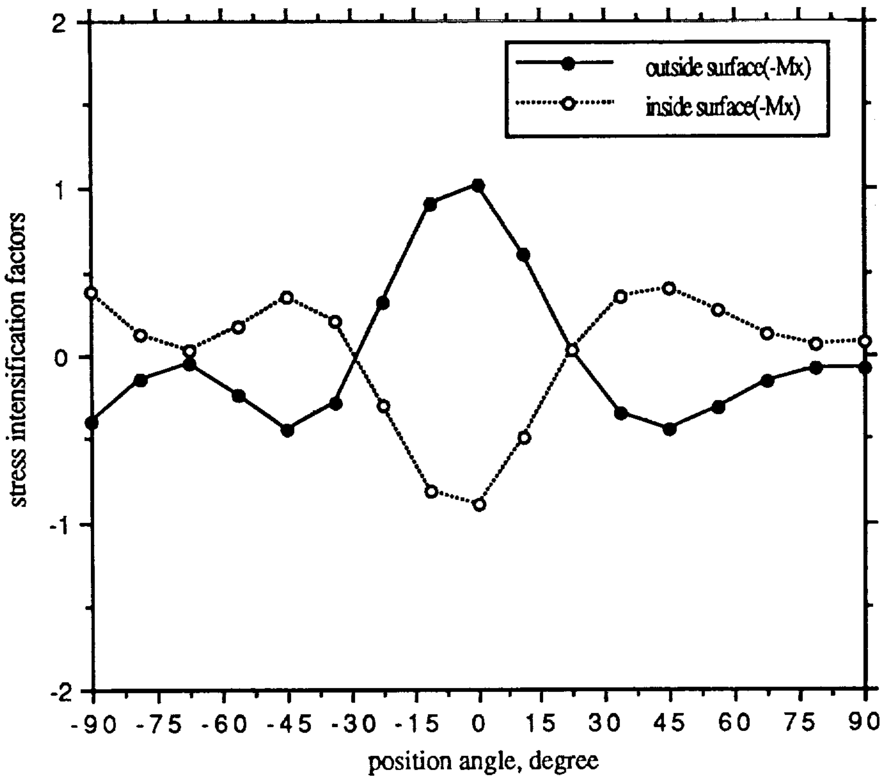

Figure 10. Shear stress factors of torsional moment at section BB.

REPORT DOCUMENTATION PAGE

Form Approved
OMB No. 0704-0188

1. AGENCY USE ONLY *(Leave blank)*	2. REPORT DATE	3. REPORT TYPE AND DATES COVERED
	June 1992	Technical Paper

4. TITLE AND SUBTITLE Effect of Type of Load on Stress Analysis of Thin-Walled Ducts	5. FUNDING NUMBERS
6. AUTHOR(S) J.B. Min and P.K. Aggarwal	
7. PERFORMING ORGANIZATION NAME(S) AND ADDRESS(ES) George C. Marshall Space Flight Center Marshall Space Flight Center, Alabama 35812	8. PERFORMING ORGANIZATION REPORT NUMBER M-688
9. SPONSORING/MONITORING AGENCY NAME(S) AND ADDRESS(ES) National Aeronautics and Space Administration Washington, DC 20546	10. SPONSORING/MONITORING AGENCY REPORT NUMBER NASA TP-3248

11. SUPPLEMENTARY NOTES
Prepared by the Structures and Dynamics Laboratory, Science and Engineering Directorate.

12a. DISTRIBUTION/AVAILABILITY STATEMENT	12b. DISTRIBUTION CODE
Unclassified—Unlimited Subject Category: 39	

13. ABSTRACT *(Maximum 200 words)*

The standard procedure for qualifying the design of duct (pipe) systems in the space shuttle main engine (SSME) has been fairly well defined. However, since pipe elbows are quite common and important in the SSME duct systems, a clear understanding of the detailed stress profile of the components is necessary for accurate structural and life assessments. This study was initiated to predict the stress profile at/near the tangent point along the cross section of the duct under various types of loads. Also, this study was further extended to understand the stiffening effect on stresses due to pressure at the tangent point. The intention of this study was to identify the importance of selecting proper locations for mounting strain gauges and to utilize the obtained results to anchor dynamic models for accurate structural and life assessments of the SSME ducts under dynamic environment. The finite element method was utilized in this study.

14. SUBJECT TERMS	15. NUMBER OF PAGES
Stress Analysis, Space Shuttle Main Engine, Thin-Walled Pipes (Ducts), Finite Element Method, Strain Gauges, Shells	20
	16. PRICE CODE A03

17. SECURITY CLASSIFICATION OF REPORT	18. SECURITY CLASSIFICATION OF THIS PAGE	19. SECURITY CLASSIFICATION OF ABSTRACT	20. LIMITATION OF ABSTRACT
Unclassified	Unclassified	Unclassified	Unlimited

NSN 7540-01-280-5500

Standard Form 298 (Rev 2-89)
Prescribed by ANSI Std. Z39-18
298-102

NASA-Langley, 1992